Journal of Catalysis **202,** 340–353 (2001)
doi:10.1006/jcat.2001.3298, available online at http://www.idealibrary.com on IDEAL®

Differences in the Reactivity of Organo-Nitro and Nitrito Compounds over Al_2O_3-Based Catalysts Active for the Selective Reduction of NO_x

Virginie Zuzaniuk,†,[1] Frederic C. Meunier,‡,[1] and Julian R. H. Ross*

*Centre for Environmental Research, University of Limerick, Limerick, Ireland; †Laboratorium für Technische Chemie, Eidgenössische Technische Hochschule Zürich, Zurich, Switzerland; and ‡School of Chemistry, The Queen's University of Belfast, Belfast, Northern Ireland

Received February 26, 2001; revised June 4, 2001; accepted June 7, 2001

The reactivity of nitromethane and *tert*-butyl nitrite, used as "models" of possible intermediates of the SCR of NO by hydrocarbons, was studied over γ-Al_2O_3, 1.2wt%Ag/Al_2O_3, 10wt%Ag/Al_2O_3, and 0.4wt%Co/Al_2O_3. DRIFTS measurements revealed the presence of formate, cyanide, and isocyanate species on the surface of γ-alumina, 1.2wt%Ag/Al_2O_3, and 0.4wt%Co/Al_2O_3 upon nitromethane adsorption, while nitrate species arose on these materials following the adsorption of *tert*-butyl nitrite. The oxidation of nitromethane over alumina, 1.2wt%Ag/Al_2O_3, and 0.4wt%Co/Al_2O_3 yielded NH_3 as the main primary product of reaction, while NO and NO_2 were formed at low temperatures during the oxidation of *tert*-butyl nitrite over the same materials. The mechanism derived from this study and from the observation that the formation of NO_2 during the C_3H_6-SCR of NO over γ-Al_2O_3 and 0.4wt%Co/Al_2O_3 was not achieved through the direct oxidation of NO by O_2 was therefore suggested. The formation of N_2 over γ-Al_2O_3, 1.2wt%Ag/Al_2O_3, and 0.4wt%Co/Al_2O_3 was proposed to occur through the reaction of organo-nitro and nitrito compounds and their derivatives. The presence of a low loading of silver appeared to favour the formation of organo-nitro compounds, while cobalt seemed to promote the formation of organo-nitrite compounds.

Key Words: **organo-nitro compounds; organo-nitrite compounds; alumina; DRIFTS; SCR of NO.**

1. INTRODUCTION

In recent years, the ever-growing interest in the removal of NO_x by selective catalytic reduction of NO_x with hydrocarbons (HC-SCR) resulted in numerous studies focusing on the mechanism of the above-cited reaction (1–17). From the studies undertaken, different mechanistic pathways have been proposed for the HC-SCR of NO_x. One of the several reaction schemes involves the formation of nitrogen-containing organic compounds as a precursor to N_2 formation (12–17). For example, Tanaka *et al.* (12) have investigated the SCR of NO with propene over Pt/SiO_2 and suggested a mechanism in which the hydrocarbon reacts with NO_2 (formed by NO oxidation) to generate some nitro/nitrite intermediates. The latter can then either react with O_2 to form N_2 or be transformed to carbonyl species, which further react with NO_2 to produce N_2. Bamwenda and co-workers (13) investigated the C_3H_6-SCR of NO over Rh/Al_2O_3 using the DRIFTS technique and reported the presence of adsorbed hydrocarbons, isocyanates (−NCO), cyanides (−CN), carboxylates (CO_3^{2-}), and nitrosonium cations ($-NO^+$) on the catalyst surface. The authors suggested that an isocyanate species was one of the intermediates in the C_3H_6-SCR of NO. Ukisu and co-workers (14) have carried out *in situ* FTIR experiments using Ag/Al_2O_3 and have observed that isocyanate bands appeared on the catalyst surface after exposure to a mixture of NO, O_2, and ethanol at room temperature and subsequently heating to 300°C. The authors suggested that the high efficiency of the C_2H_5OH-SCR of NO_x in the presence of water is due to the formation of large concentrations of surface isocyanate intermediates.

Various studies were carried out on the reactivity of different nitrogen-containing organic compounds in connection with the HC-SCR of NO_x, these investigations helping to identify and clarify the possible involvement of such species as reaction intermediates in the HC-SCR (12, 18–22). Cowan *et al.* and Cant *et al.* (18, 19) studied the gas phase decomposition and oxidation of nitromethane and its reactivity over different catalysts such as Co−ZSM5, H−ZSM5, Na−ZSM5, SiO_2, or Al_2O_3 in connection with the SCR of NO_x. They found that nitromethane decomposed to NH_3 and/or HNCO depending on the catalyst and conditions used. The authors suggested that NO_2 could facilitate the desorption of strongly adsorbed decomposition products, HNCO and NH_3, since the reaction of NH_3 with NO_2 was very fast over Co−ZSM5 and gave N_2 as the major product. Obuchi and co-workers (20) have studied the reactivity of *tert*-butyl-substituted nitrogen compounds over alumina. They have investigated the catalytic decomposition, oxidation, and reaction of *tert*-butyl N-oxide (t-CNO), *tert*-butyl isocyanate (t-NCO), and *tert*-butyl cyanide (t-CN) with $NO_2 + O_2$ or $NO + O_2$. They concluded that once nitrile N-oxides are formed under

[1] To whom correspondence should be addressed. Fax: +41 (0)1 6321162. E-mail: zuzaniuk@tech.chem.ethz.ch. E-mail: f.meunier@qub.ac.uk.

0021-9517/01 $35.00

HC-SCR conditions, they are readily converted to N_2 through several reaction steps. Yamaguchi (21) studied the adsorption of nitromethane on Al_2O_3 using infrared spectroscopy, NMR spectroscopy, and TPD. Nitromethane decomposed to isocyanate, which further led to the formation of ammonia and urea on the catalyst surface at 473 K. Yamaguchi suggested that these reaction products (isocyanate and ammonia), formed from the decomposition of organic nitro compounds, could then react with nitrogen oxides during the HC-SCR of NO. Kameoka *et al.* (22) undertook similar investigations, studying the adsorption of nitromethane and nitroethane on the nonpromoted metal oxides Al_2O_3 and TiO_2 as well as on metal-oxide-supported silver catalysts, namely, 2wt%Ag/Al_2O_3, Ag/TiO_2, and Ag/SiO_2, using infrared spectroscopy. They also observed the formation of adsorbed isocyanate (NCO) species on the catalyst surface under certain conditions. The authors suggested that the formation of those species mainly occurred on the Lewis acid sites of the oxide support, silver promoting the activation of nitroethane by a scission of C–C bonds and/or the rearrangement reaction of adsorbed NCO species. Kameoka and co-workers also carried out separate SCR experiments using ethanol as the reducing agent and concluded that the efficiency of supported silver catalysts in NO_x reduction with ethanol was correlated with the nature of the isocyanate surface species arising from the thermodecomposition of organic nitro compounds.

While organic nitro or nitrite have usually been considered as a whole as far as their involvement in SCR reaction is, our group previously reported (23) that the reactivity of nitro alkanes and *tert*-butyl nitrite over Al_2O_3 showed significant differences, stressing the need to consider differently the role of these compounds. This is of particular importance with regard to some results previously reported by our group on the C_3H_6-SCR of NO over Al_2O_3-based materials (24–26): high yields of NO_2 (in excess of the thermodynamic limit associated with the direct oxidation of NO to NO_2 by O_2) were obtained over unpromoted-alumina and 0.4%Co/Al_2O_3. A reaction mechanism involving the formation and combustion of organo-nitrogen compounds from the reaction of C_3H_6, NO, and O_2 was suggested to explain the formation of NO_2 during the SCR reaction. In an attempt to clarify the type of organo-nitrogen species from which NO_2 could originate during the C_3H_6-SCR of NO over Al_2O_3-based materials, the study of the reactivity of organo-nitro and -nitrite compounds was extended to Ag- and Co-promoted alumina materials active for the C_3H_6-SCR of NO (24–26).

2. EXPERIMENTAL

2.1. Catalyst Preparation and Characterisation

The γ-Al_2O_3 utilised in this work was supplied by Alcan (AA400). For the preparation of the silver-promoted materials, an appropriate amount of silver nitrate (analytical grade, Johnson Matthey) was dissolved in a volume of deionised water equal to that of the porous volume of the alumina. The solutions were then deposited on the alumina by dry impregnation at room temperature. The samples were dried for 14 h at 120°C and then calcined at 600°C for 2 h in synthetic air. For the preparation of the cobalt-promoted catalyst, a similar procedure was applied using a cobalt acetate tetrahydrate salt (analytical grade, Aldrich). N_2 adsorption at 77 K using a Micromeretics system was used to measure the surface area of the samples. Prior to these measurements, the samples were each outgassed for 2 h at 200°C under a dynamic vacuum (i.e., with a residual pressure lower than 20 Pa). Atomic absorption spectroscopy measurements were performed to determine the promoter content of the catalysts. The loadings of promoters on the alumina are reported in weight percent.

2.2. Catalytic Tests

A quartz flow microreactor (3-mm internal diameter) was used for the catalytic tests, the catalytic bed being held in place by quartz wool plugs. Two hundred milligrams of catalyst was loaded in the reactor for all the experiments reported here. The temperature of reaction was measured inside the reactor, just before the catalyst bed, by a thermocouple enclosed in a quartz tube. The temperature of the reactor furnace was reduced from 600 to 100°C in 50°C intervals dwelling at each temperature for 1 h. The data points reported were taken in the last 20 min of the dwelling stage at each temperature. The actual feed compositions used in each of the experiments reported in this paper are shown in the legends of the appropriate figures. Nitromethane (Fluka, puriss ≥99.0%) and *tert*-butyl nitrite (Fluka, assay ≥90%) were fed using a saturator flushed by a He stream; this stream was then added to a flow of the other reactants. The total flow rate was 100 ml min^{-1}. The saturator was kept at room temperature or 0°C for the experiments using nitromethane or *tert*-butyl nitrite, respectively.

Analysis of the reaction products was carried out using a Nicolet 550 FT-IR spectrophotometer fitted with a gas cell of volume 0.22 dm^3 and a triglycine sulphate pyroelectric (DTGS) detector. A total of 64 scans was recorded at a resolution of 1 cm^{-1}. The concentration of a given species was measured by integrating the peaks in selected regions of its absorbance spectrum and comparing these to a calibration curve. A Varian 3400CX gas chromatography, equipped with a 2-m-length molecular sieve 5A column and using a TCD detector, was used to detect and quantify N_2.

2.3. Diffuse Reflectance FT-IR Analysis

The diffuse reflectance FT-IR measurements were carried out *in situ* in a high-temperature cell (Spectra-Tech) fitted with ZnSe windows. The sample for study (ca. 30 mg) was finely ground and placed in a ceramic crucible, the

temperature of which could be varied from 20 to 800°C. All the samples were calcined *in situ* at 630°C prior to analysis.

The nitro compounds (Fluka), namely, nitromethane (puriss ≥99.0%), nitroethane, nitrobutane, and 2-nitropropane, and nitrite compounds (Fluka), e.g., *n*-butyl nitrite and *tert*-butyl nitrite (assay ≥90%), were fed using a saturator flushed by a He stream for 30 min. The saturator was then by-passed and the temperature of the sample was increased from room temperature in 100°C steps, dwelling for 1 h at each temperature. For the experiments involving the adsorption of the organo-nitrite compounds, the saturator temperature was kept at 0°C; for the organo-nitro molecules, the temperature was 20°C. In all cases, the total flow rate was 100 ml min^{-1}. The absorbance measured after the reaction stream passed over the catalyst relative to that of the same material at the same temperature under a stream of argon (background) is reported for each spectrum. Spectra were recorded using 128 scans at a resolution of 2 cm^{-1}.

3. RESULTS AND DISCUSSION

3.1. The Reactivity of Nitromethane and tert-Butyl Nitrite over γ-Al_2O_3-Based Materials

Figure 1 shows the concentrations of the main nitrogen-containing products of the oxidation of nitromethane over γ-Al_2O_3 (148 $m^2\,g^{-1}$) as a function of temperature. NO, N_2, N_2O, NH_3, and traces of HCN (not quantified) were detected. No NO_2 was produced at any temperature. NH_3 was the main product of reaction at temperatures below 550°C and its maximum yield occurred in the temperature range 250–400°C. At temperatures above 400°C, the NH_3 concentration decreased steadily until it was undetectable at 600°C; at the same time, the formation of NO and N_2 increased, reaching a maximum at 600°C. HCN was detected over the temperature range 100–400°C; above 400°C, no HCN could be detected. No CO was detected and CO_2 was the main C-containing product detected.

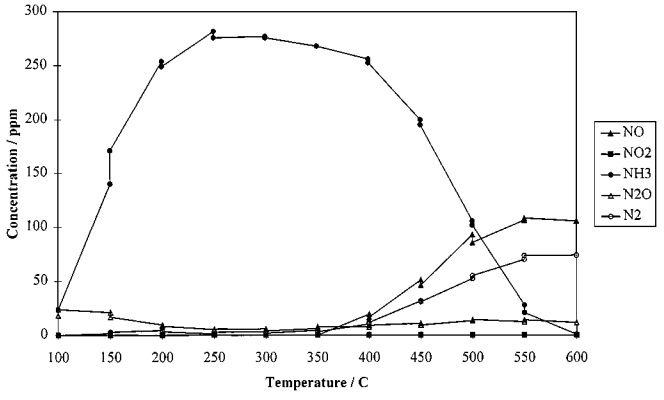

FIG. 1. Catalytic activity of alumina in the oxidation of nitromethane as a function of temperature. Feed: 0.03%CH_3NO_2 + 1.5%O_2 in He. $M(Al_2O_3)$ = 200 mg. Total flow = 100 ml min^{-1}.

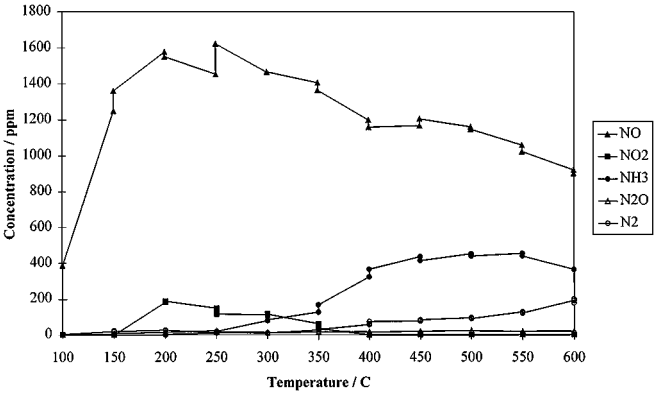

FIG. 2. Concentrations of various N-containing products formed during the oxidation of *tert*-butyl nitrite on alumina as a function of temperature. Feed: 0.2% $C(CH_3)_3ONO$ + 1.5% O_2 in He. $M(Al_2O_3)$ = 200 mg. Total flow = 100 ml min^{-1}.

Both nitromethane (Fig. 1) and *tert*-butyl nitrite (Fig. 2) were very reactive under the conditions used here, and at 200°C and above, the conversions of both compounds were total. While the oxidation of nitromethane yielded NH_3 as the main reaction product, the oxidation of *tert*-butyl nitrite led mainly to the formation of the nitrogen oxides NO and NO_2.

Figure 2 shows the concentrations of the main nitrogen-containing products of the oxidation of *tert*-butyl nitrite over Al_2O_3 as a function of temperature. NO, NO_2, N_2, N_2O, NH_3, and HCN (not quantified) were detected. NO was the main product of reaction over the whole temperature range investigated, i.e., 100–600°C; its concentration passed through a maximum at 200°C before steadily decreasing with increasing temperature. NO_2 was the second most abundant product of the reaction between 200 and 300°C, but its concentration decreased rapidly toward zero at 400°C. On the other hand, NH_3 could be detected for temperatures above 300°C and it became the second most abundant product above 300°C. A small amount of N_2 could also be detected at high temperatures, its maximum concentration occurring at 600°C, while a very low concentration of N_2O could also be detected above 100°C.

Over alumina, the reaction of nitromethane in the presence of O_2 yielded NH_3, which was formed as a result of the thermal decomposition of the starting molecule, this being the main primary product of reaction. Increasing the temperature led to the oxidation of the NH_3 to produce NO and N_2. In contrast, the oxidation of *tert*-butyl nitrite yielded NO and (to a lower extent) NO_2 as main primary products of reaction at low temperatures. At higher temperatures, NO_2 could no longer be detected in the gas stream, and this was attributed to its reduction by isobutene (formed as product of reaction) to produce

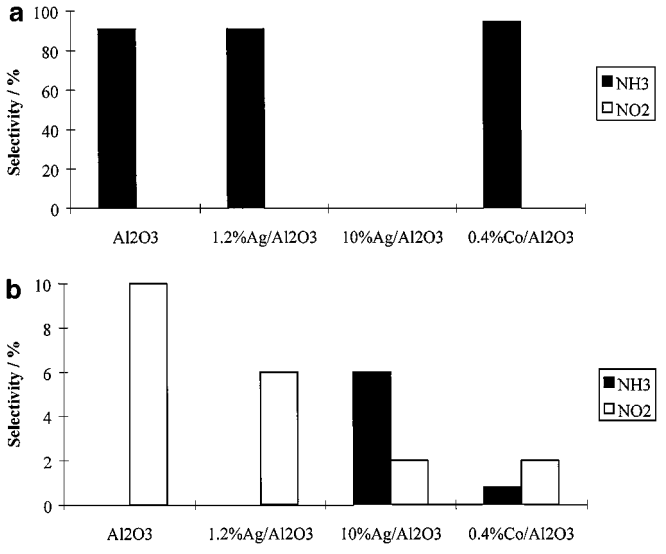

FIG. 3. Comparison of the selectivities to NO_2 and NH_3 over Al_2O_3, 1.2% Ag/Al_2O_3, 10% Ag/Al_2O_3, and 0.4% Co/Al_2O_3 during the oxidation of nitromethane (a) and *tert*-butyl nitrite (b) at 200°C. M(catalyst) = 200 mg. Total flow = 100 ml min^{-1}.

NH_3 or/and N_2. It is noteworthy that NO_2 was mainly not observed when NH_3 was present in the reaction products and vice versa. This feature was also observed during the oxidation of nitromethane and *tert*-butyl nitrite over the other catalysts under investigation, namely, 1.2% Ag/Al_2O_3 (141 m^2 g^{-1}), 10% Ag/Al_2O_3 (120 m^2 g^{-1}), and 0.4% Co/Al_2O_3 (135 m^2 g^{-1}), with the exception of the oxidation of *tert*-butyl nitrite over 10% Ag/Al_2O_3. This is illustrated in Fig. 3, which shows a comparison of the selectivity to NH_3 and NO_2 obtained at 200°C for the oxidation of nitromethane (Fig. 3a) and *tert*-butyl nitrite (Fig. 3b) over γ-Al_2O_3, 1.2% Ag/Al_2O_3, 10% Ag/Al_2O_3, and 0.4% Co/Al_2O_3. At 200°C, no NO_2 was detected over any of the four catalysts investigated, while NH_3 was the main reaction product over γ-Al_2O_3, 1.2% Ag/Al_2O_3, and 0.4% Co/Al_2O_3 with a selectivity above 90%. Over 10% Ag/Al_2O_3, neither NH_3 nor NO_2 were detected at this temperature, N_2O being the main reaction product. In contrast, during the oxidation of *tert*-butyl nitrite at 200°C, NO_2 was detected over the four catalysts along with NO, no NH_3 being produced over unpromoted alumina and 1.2% Ag/Al_2O_3. The 10% Ag/Al_2O_3 material seemed again to exhibit different behaviour from the other catalysts as NH_3 and NO_2 were both detected at 200°C during the reaction of *tert*-butyl nitrite with O_2. It clearly appears from those results that organo-nitro and organo-nitrite compounds reacted in a different way: while organo-nitro species mainly yielded NH_3, organo-nitrite compounds could yield more NO_2.

Cant *et al.* (19) reported that temperatures above 450°C were required for nitromethane to react in the gas phase, while Otsuka *et al.* (27, 28) suggested that organo-nitrito species were important intermediates in the gas phase oxidation of light alkanes in the presence of NO. Hence, the occurrence of gas phase reactions possibly triggered by the catalyst surface cannot be excluded. However, the results obtained here over the different catalysts appear to result from the different activities of the materials themselves, especially at the lower temperatures.

3.2. *DRIFT Spectra on γ-Al_2O_3*

Figure 4 shows the DRIFT spectra of the species formed from the adsorption of nitromethane (NM) on Al_2O_3. Bands assigned to physisorbed nitromethane (1380, 1407, 1572, and 2959 cm^{-1}), together with peaks at 1259, 1285, 1431, 3067, and 3192 cm^{-1}, were observed on the alumina surface at room temperature. At 100°C, physisorbed nitromethane had completely desorbed from the surface while peaks at 1259, 1285, 1387, 1533, 1598, 2231, and 2250 cm^{-1} were detected. In accordance with the results reported by Yamaguchi (21), the peaks at 1259, 1285, 1598, 3067, and 3192 cm^{-1} can be assigned to the aci-anion of nitromethane ($CH_2NO_2^-$), this being produced from the dissociative adsorption of nitromethane on the alumina surface. The peaks at 2231 and 2250 cm^{-1} may arise from an (inorganic) isocyanate group, a bridged cyanide, or a nitrile species (29, 30). Two bands at 2228 and 2250 cm^{-1} were observed when cyclohexyl isocyanate was adsorbed on alumina (not shown) and additional experiments have shown that the bands at 2228 and 2250 cm^{-1} derived from nitromethane were readily displaced by water at 300°C, NH_3

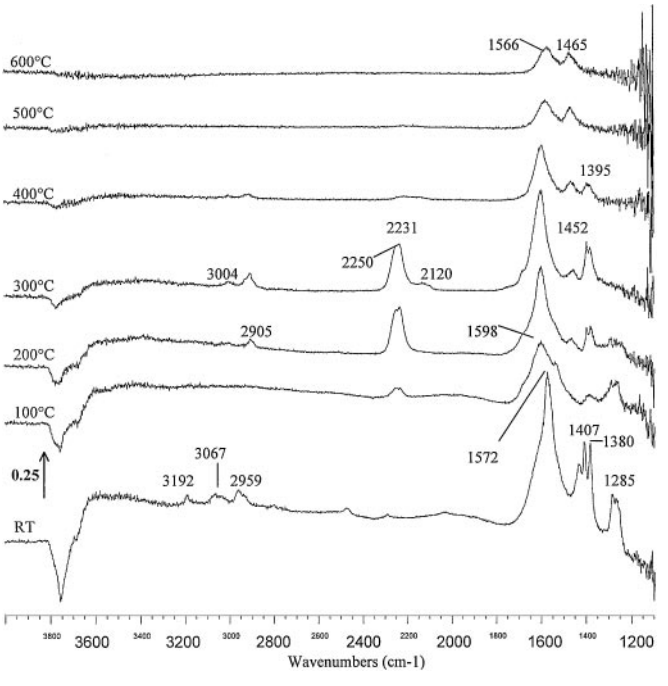

FIG. 4. *In situ* DRIFT spectra of the surface species resulting from the adsorption of nitromethane on alumina. Total flow = 100 ml min^{-1}.

being observed in the gas phase. This high reactivity with water suggests that these bands should be assigned to an isocyanate species rather than to a cyanide/nitrile species since the latter would be significantly less reactive toward water (20, 31). Therefore, and in agreement with previously reported results (32), the peaks at 2231 and 2250 cm^{-1} are assigned to anionic isocyanate (NCO^-) and covalent isocyanate (NCO), respectively. The peaks at 1387 and 1532 cm^{-1} could only be detected at 100°C. Yamaguchi (21) has reported the presence of a peak at 1532 cm^{-1} on his alumina surface during the adsorption of nitromethane and assigned it to a (C, N, O) adduct along with other peaks that do not appear to be formed on the alumina used in this work. That these peaks at 1387 and 1532 cm^{-1} appear at 100°C and then disappear at 200°C, at which the intensity of the isocyanate peaks increases suggests that these peaks may be due to a precursor responsible for the formation of isocyanate species. The exact nature of this precursor is difficult to determine from the present results and additional experiments, possibly using labeled reactants, should be carried out to confirm the assignment. However, these two peaks are tentatively assigned to the ν(CN) and δ(CNH) vibrations, respectively, of formohydroxamic acid (CHO–N(H)OH), which has already been suggested as a possible intermediate in the reactivity of nitromethane over different zeolites. Increasing the temperature to 200°C resulted in a decrease of the bands assigned to the aci-anion of nitromethane and to their complete disappearance at 300°C. The intensity of the bands assigned to surface isocyanate species increased with increasing the temperature to reach a maximum at 300°C before decreasing at higher temperature and completely disappearing at 500°C. At 200°C, new bands appeared on the alumina surface at 1377 cm^{-1} (ν^{s}_{OCO}), 1395 cm^{-1} (δ_{CH}), 2905 cm^{-1} (ν_{CH}), and 3004 cm^{-1} (combination band $\nu^{a}_{OCO} + \delta_{CH}$); these, together with the band at 1598 cm^{-1} (ν^{a}_{OCO}), can be assigned to a formate species (29, 33). Other peaks were detected at 1452 and 1682 cm^{-1} on the sample surface at 200 and 300°C and they are tentatively assigned to the ν_{NCO} and ν_{CO} vibrations of carbamic acid (NH_2COOH), respectively. The band at 1452 cm^{-1} could also be assigned to the ammonium species NH_4^+ resulting from the adsorption of NH_3 (produced from the thermal decomposition of NM) on the Brönsted sites of the alumina (34). The small band appearing at 2120 cm^{-1} at 300°C could be characteristic of a linearly adsorbed cyanide. The adsorption of HCN on the Al_2O_3 used in this work (not shown) gave only a band at 2092 cm^{-1} in the spectral region 2000–2300 cm^{-1}. Increasing the temperature to 400°C resulted in a decrease of the peak intensities of the formate bands and to the appearance of a band at 1465 cm^{-1}, which can be assigned to a carboxylate species. At 500 and 600°C, the carboxylate species, with characteristic bands at 1465 and 1566 cm^{-1}, was the only detectable entity on the alumina surface.

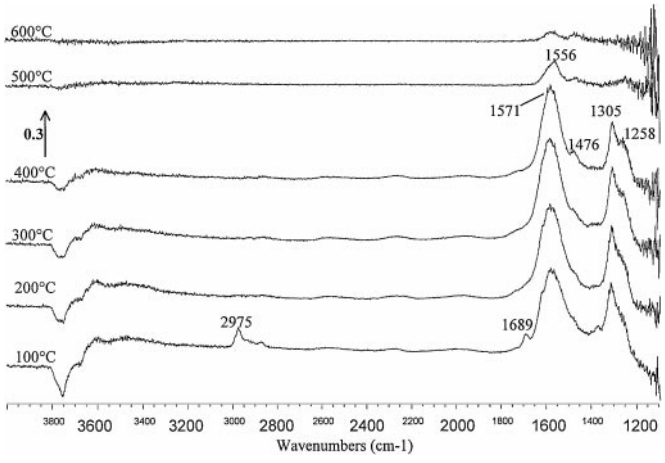

FIG. 5. *In situ* DRIFT spectra of the surface species resulting from the adsorption of *tert*-butyl nitrite on alumina. Total flow = 100 ml min^{-1}.

Figure 5 shows the DRIFT spectra obtained from the adsorption of *tert*-butyl nitrite on Al_2O_3. The results were markedly different from those obtained using nitromethane (Fig. 4) and other organic nitro compounds (Fig. 7). At 100°C, main bands were detected on the alumina surface at 1305 and 1571 cm^{-1}, along with smaller peaks at 1258, 1368, 1689, 2875, and 2975 cm^{-1}. The bands at 1258, 1305, and 1571 cm^{-1}, which remained on the surface up to 400°C, could be assigned to nitrate species; the band at 1571 cm^{-1} probably resulted from an overlapping of two bands at 1555 and 1586 cm^{-1}. Separate adsorption experiments over the same Al_2O_3 using NO, NO_2, and O_2 showed that the bands at 1258 and 1555 cm^{-1} were coupled, whereas the band at 1305 cm^{-1} was coupled to a band at 1586 cm^{-1}. According to the literature, these bands correspond to two different types of bidentate nitrate species (35). The peaks observed at 100°C at 1611 and 1689 cm^{-1} are characteristic of the N=O stretching vibrations of organic nitrite compounds and could be related to physisorbed *tert*-butyl nitrite, together with the CH stretching vibrations (at 2875 and 2975 cm^{-1}) observed at room temperature (not shown) and 100°C. These bands decreased with increasing temperature and disappeared at 200°C and only the ad-NO_x species bands remained on the sample surface at this temperature. At 400°C, carboxylate species (band at 1476 cm^{-1}) appeared on the catalyst surface. At 600°C, only traces of carboxylate species (bands at 1476 and 1571 cm^{-1}) remained on the sample surface.

The adsorption of n-BuONO on alumina was also carried out and the results are reported in Fig. 6 for temperatures ranging from room temperature to 600°C. Bands in the C–H stretching vibration region (2879, 2940, and 2966 cm^{-1}) were observed up to 600°C. This result is markedly different from what was observed during the adsorption of t-BuONO over Al_2O_3, in which case the bands corresponding to the

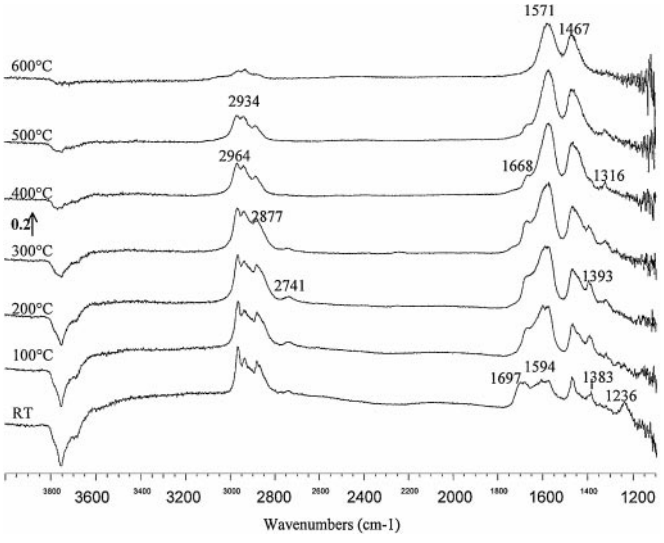

FIG. 6. *In situ* DRIFT spectra of the surface species resulting from the adsorption of *n*-butyl nitrite on alumina. Total flow = 100 ml min^{-1}.

ν(C–H) vibrations had already disappeared from the surface at 200°C. The linear organic nitrite was adsorbed much more strongly on the alumina surface, possibly due to its oligomerisation. At room temperature, a peak characteristic of an inorganic nitrite species was detected at 1236 cm^{-1} (35). Increasing the temperature resulted in the disappearance of this peak and in the appearance of a peak at 1310 cm^{-1}, assigned to an inorganic nitrate species (29, 35, 36). C-containing species were also detected on the alumina surface, with the peaks at 1466 and 1571 cm^{-1} assigned to carboxylate species. At the lower temperatures, however, the band at 1571 cm^{-1} was quite broad and probably resulted from the overlapping of several peaks. Among others, it would be quite possible that the peak at 1580 cm^{-1}, usually associated with the nitrate band at 1310 cm^{-1}, was present here. As in the case of *tert*-butyl nitrite (Fig. 5), essentially no isocyanate species were detected at any temperature for n-BuONO, while those species could be detected with all nitro compounds studied, namely, nitromethane (Fig. 4), nitroethane, nitrobutane, and 2-nitropropane (Fig. 7).

Figure 7 shows the DRIFT spectra of surface species resulting from the adsorption at room temperature of nitroethane, nitrobutane, and 2-nitropropane on alumina followed by heating to 300°C in argon alone. Despite the differences in the alkyl chain associated with the nitro groups, similar DRIFT spectra to those observed with nitromethane, were obtained with all three of these organo-nitro compounds. In particular, all three nitro compounds gave rise to isocyanate species with a broad band, probably resulting from the overlapping of the characteristic bands at 2230 and 2250 cm^{-1} (32) arising in the 2220- to 2250-cm^{-1} region. Bidentate formate species, with the bands at ca. 1394 and 1595 cm^{-1}, could also be observed with the three compounds. The band at ca. 1460 cm^{-1} could be assigned to the $\nu^s(CO_2^-)$ vibration of a carboxylate species or/and to the δ(CH) vibration of the alkyl groups since both species could be formed on the alumina surface under the experimental conditions used here. Unidentate formates or/and unidentate acetates were also present on the alumina surface following the adsorption of nitroethane, with characteristic peaks at 1339 and 1675 cm^{-1}. Equivalent unidentate formate/acetate species were probably also produced on the alumina surface following the adsorption of nitrobutane and 2-nitropropane, but in smaller concentration since a shoulder could be observed on the main peak at around 1585–1590 cm^{-1} in both cases. The assignment of the peaks at 1339 and 1675 cm^{-1} to unidentate formate/acetate species result from separate experiments (not shown) in which formic acid and acetic acid were fed to alumina at room temperature using a saturator. The latter was then by-passed and the temperature was increased. Bands in the C–H stretching vibration region (2800–3200 cm^{-1}) were also observed in the three spectra, these being characteristic of the corresponding alkyl groups.

Contrary to the case of the organo-nitrite species, no inorganic nitrate and/or nitrite species were detected at any time and/or temperature when organo-nitro compounds were adsorbed on the alumina surface.

3.3. *DRIFT Spectra on 1.2% Ag/Al_2O_3*

Figure 8 shows the DRIFT spectra of the species formed from the adsorption of nitromethane on 1.2% Ag/Al_2O_3. Surface species similar to those arising on alumina (Fig. 4) were observed at 100°C: the peaks observed at 1258 and 1284 cm^{-1} were previously assigned to the aci-anion of nitromethane ($CH_2NO_2^-$) and these appeared together

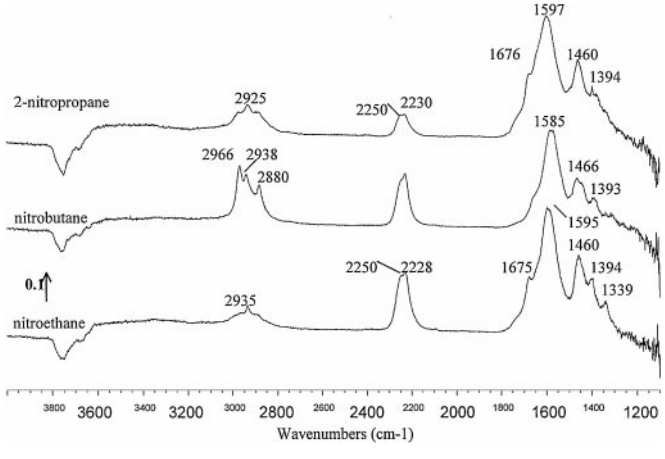

FIG. 7. *In situ* DRIFT spectra of the surface species resulting from the adsorption at room temperature of nitroethane, nitrobutane, and 2-nitropropane on alumina and subsequently heating in Ar to 300°C. Total flow = 100 ml min^{-1}.

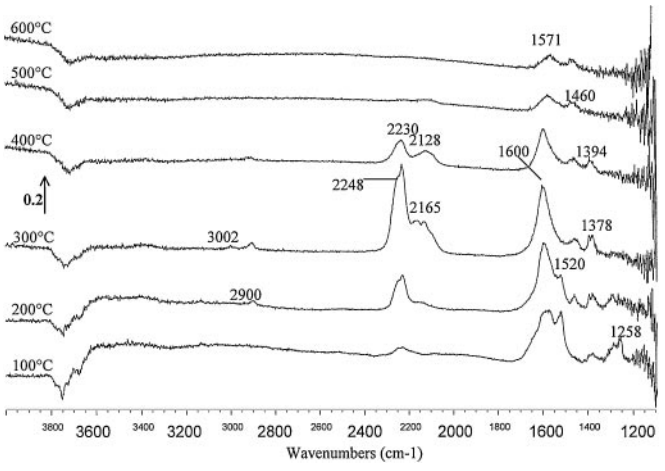

FIG. 8. *In situ* DRIFT spectra of the surface species resulting from the adsorption of nitromethane on 1.2% Ag/Al_2O_3. Total flow = 100 ml min^{-1}.

with peaks at 2230 and 2248 cm^{-1} characteristic of ionic and covalent isocyanate species, respectively. The peaks at 1383 and 1520 cm^{-1}, thought to characterise an isocyanate precursor (possibly formohydroxamic acid), were also observed. The intensity of the bands assigned to the aci-anion of nitromethane decreased upon increasing temperature and eventually disappeared at 300°C. In contrast, the concentration of surface isocyanate species increased with increasing temperature to reach a maximum at 300°C. Upon heating to 400°C, their concentration decreased but they could still be observed on the catalyst surface. At 200°C, a shoulder also appeared on the isocyanate peak at 2130 cm^{-1}. At 300°C, this shoulder "split" into two peaks at 2165 and 2128 cm^{-1}. The peak at 2165 cm^{-1}, which could not be observed during the adsorption of nitromethane on unpromoted alumina (Fig. 4), is tentatively assigned to the stretching vibration of a cyanide species (ν(CN)) adsorbed on a Ag site. At 400°C, the intensity of the peaks assigned to the cyanide species decreased, but the rate of decrease was much lower than in the case of the isocyanate bands. From 200 to 400°C, formate species were observed on the surface of the 1.2% Ag/Al_2O_3 material, these having bands at 1378 cm^{-1} (ν^{s}_{OCO}), 1394 cm^{-1} (δ_{CH}), 1600 cm^{-1} (ν^{a}_{OCO}), 2900 cm^{-1} (ν_{CH}), and 3004 cm^{-1} (combination band $\nu^{a}_{OCO} + \delta_{CH}$). In contrast, the peaks observed on unpromoted alumina (Fig. 4) and assigned to carbamic acid (NH_2COOH) could not be detected in the case of 1.2% Ag/Al_2O_3. This appears to suggest that the silver particles (at low loading) promote the reaction of this carbamic acid intermediate (to give NH_3, Fig. 1). At 500 and 600°C, only carboxylate species were detectable on the alumina surface, these having characteristic bands at 1460 and 1571 cm^{-1}.

An interesting feature of the reaction of nitromethane on the Ag-promoted alumina compared to that over the unpromoted alumina was the ratio between the intensities of the isocyanate and formate bands. It can clearly be seen from the spectra at 300°C or even 400°C that the ratio A(NCO)/A(Formate) (where A represents the absorbance) is much higher over 1.2% Ag/Al_2O_3 than over alumina. This seems to indicate that the Ag promotes the formation of isocyanate species on the alumina surface. A similar observation applies to the cyanide species at both 300 and 400°C.

Figure 9 shows the DRIFT spectra of the species formed on the surface of the 1.2% Ag/Al_2O_3 sample following the adsorption of *tert*-butyl nitrite. At 100°C, bands characteristic of nitrate species and of the *tert*-butyl group of the organic nitrite compound were detected on the sample surface. The bands at 1209, 1240, 1370, 1474, 2870, and 2972 cm^{-1} can be assigned to the vibrations $\nu^{a}(C_3C)$, $\nu(CC_3)$, $\delta^{s}(CH_3)$, $\delta^{a}(CH_3)$, $\nu^{s}(CH_3)$, and $\nu^{a}(CH_3)$ of the *tert*-butyl group, respectively (30). The bands at 1255 + 1550 cm^{-1} and 1305 + 1591 cm^{-1} are assigned to two different types of nitrates, which will be referred to as nitrates "A" and "B". Increasing the temperature to 200°C resulted in the appearance of isocyanate species with a characteristic band at 2232 cm^{-1}, and the bands characteristic of nitrate species and of the stretching vibration ν(CH) of the *tert*-butyl group could still be observed. These results are very different from those obtained from the adsorption of *tert*-butyl nitrite over unpromoted alumina (Fig. 5), in which case increasing the temperature to 200°C led to the desorption of all but the surface nitrate species. Moreover, no isocyanate species could be observed in the case of alumina alone. At 300°C, the main surface species arising on 1.2% Ag/Al_2O_3 were nitrates with the peaks at 1255, 1305, and 1552 cm^{-1}, while formate species could also be detected, these having peaks at 1370 ($\nu^{s}(CO_2^-)$), 1393 (δ(CH)), and 1591 cm^{-1} ($\nu^{a}(CO_2^-)$) (29, 33). At 400°C, formate species had disappeared and carboxylate species had appeared (band at

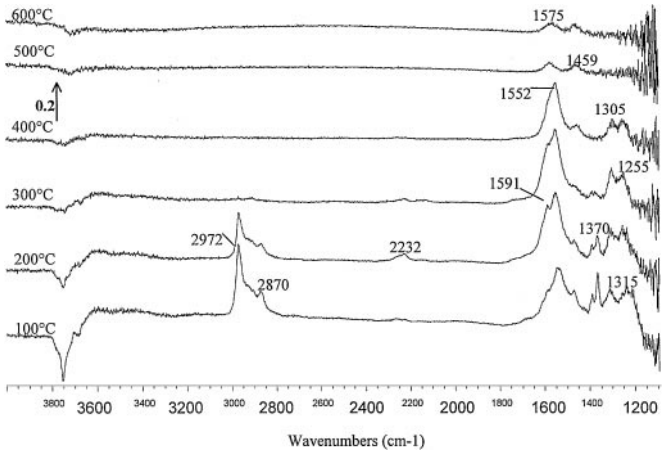

FIG. 9. *In situ* DRIFT spectra of the surface species resulting from the adsorption of *tert*-butyl nitrite on 1.2% Ag/Al_2O_3. Total flow = 100 ml min^{-1}.

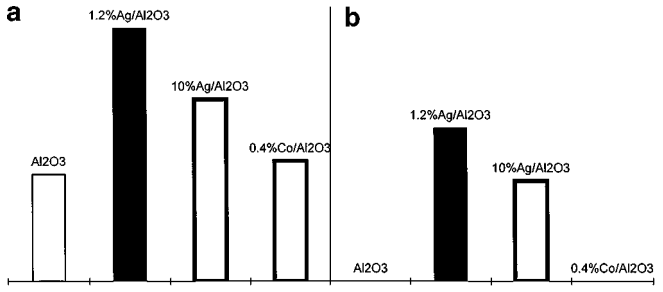

FIG. 10. Integrated area of the peak detected at 2975 cm^{-1} (ν(C–H)) at 100°C (a) and 200°C (b) during the adsorption of *tert*-butyl nitrite on Al_2O_3, 1.2% Ag/Al_2O_3, 10% Ag/Al_2O_3, and 0.4% Co/Al_2O_3. Total flow = 100 ml min^{-1}.

1459 cm^{-1}), in addition to the nitrate species. At 500 and 600°C, only carboxylate species could be detected on the sample surface.

Compared to alumina alone (Fig. 5), the surface coverage in hydrocarbons (HC) was increased at low temperatures (i.e., 100 and 200°C) over the Ag-promoted materials. This is illustrated in Fig. 10, which represents the integrated absorbance at 100°C (a) and 200°C (b) of the peaks detected between 2800 and 3000 cm^{-1} on the surface of the four catalysts under investigation. While the hydrocarbon species completely desorbed from the surface of the alumina and Co/Al_2O_3 samples at 200°C, they were still detected over the low and high silver loading materials. These results seem to indicate that one of the roles of the Ag would be to promote the adsorption of hydrocarbons, possibly by creating more adsorption sites for the HC.

Figure 11 shows the DRIFT spectra obtained at room temperature over alumina and 1.2% Ag/Al_2O_3 after 1 h under a flow containing C_3H_6 and O_2. These results highlight as well the promotional effect of the Ag particles on the adsorption of hydrocarbon species: two peaks centred at 1637 and 2957 cm^{-1} were detected over alumina and respectively assigned to the stretching vibrations ν(C=C) and $\nu^a(CH_3)$ of propene, while various bands of more intensity could be detected over 1.2% Ag/Al_2O_3. These bands at 1380, 1458, 2862, 2898, 2927, 2957, 2981, and 3082 cm^{-1} were assigned to the vibrations $\delta^s(CH_3)$, $\delta^a(CH_3)$, $2\delta^a(CH_3)$, $2\delta^a(CH_3)$, $\nu^s(CH_3)$, $\nu^a(CH_3)$, $\nu^s(CH_2)$, and $\nu^a(CH_2)$ of physisorbed propene, respectively.

3.4. *DRIFT Spectra on 10% Ag/Al_2O_3*

Figure 12 shows the DRIFT spectra of the species formed from the adsorption of nitromethane on 10% Ag/Al_2O_3. At 100°C, peaks at 1567, 1600, 2154, and 2240 cm^{-1} were observed on the sample surface. A wide plateau also appeared between 1250 and 1370 cm^{-1}; however, the peak resolution was poor and it was difficult to distinguish any peak in this region. It should be noted that, at low temperature (100°C) over 10% Ag/Al_2O_3, the formation of cyanide species (with

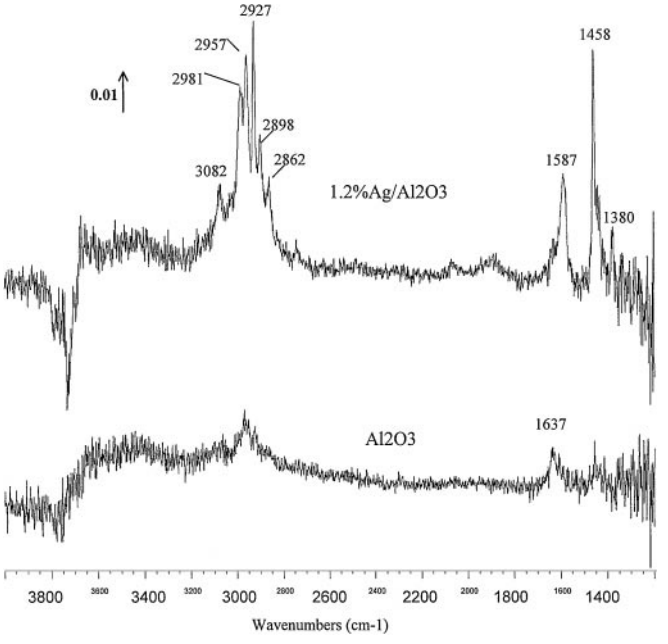

FIG. 11. *In situ* DRIFT spectra resulting from the adsorption of C_3H_6 in the presence of O_2 at room temperature. Feed: 0.05% C_3H_6 + 2.5% O_2 in Ar. Total flow = 100 ml min^{-1}.

a peak at 2154 cm^{-1}) was favoured over that of isocyanate species (peak at 2240 cm^{-1}) and that this contrasts the reaction on the unpromoted alumina or low silver loading alumina samples. At 200°C, formate species could be detected on the sample surface (peaks at 1378, 1395, 1600, and 2905 cm^{-1}) along with isocyanate species with a peak at 2240 cm^{-1}, the intensity of which increased with temperature. Carboxylate species, with the peaks at 1459 and 1567 cm^{-1}, also appeared at 200°C on the catalyst surface and these remained the only surface species at 500 and 600°C. The isocyanate and cyanide species disappeared almost completely from the sample surface at 400°C.

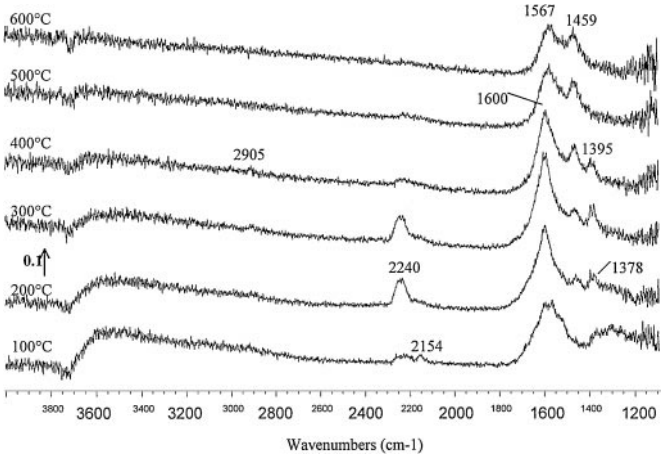

FIG. 12. *In situ* DRIFT spectra of surface species resulting from the adsorption of nitromethane on 10% Ag/Al_2O_3. Total flow = 100 ml min^{-1}.

TABLE 1

Assignment of the Bands Resulting from the Adsorption of Nitromethane (NM) on the Alumina-Based Materials (s = Symmetric, a = Asymmetric, ν = Stretching, δ = Bending, RT = Room Temperature)

Wavenumber (cm^{-1})	Surface species	Vibration	Temperature (°C)
1259	$CH_2NO_2^-$	$\nu^a(NO_2)$	RT to 200
1285	$CH_2NO_2^-$	$\nu^a(NO_2)$	RT to 200
1377	Formate	$\nu^s(CO_2^-)$	200 to 400
1380	Physisorbed NM		RT
1387	Formohydroxamic acid	ν(CN)	100
1395	Formate	δ(CH)	200 to 400
1407	Physisorbed NM		RT
1452	Carbamic acid	ν(NCO)	200 to 300
1465	Carboxylate	$\nu^s(CO_2^-)$	400 to 600
1533	Formohydroxamic acid	δ(CNH)	100
1566	Carboxylate	$\nu^a(CO_2^-)$	600
1572	Physisorbed NM		RT
1575	Carboxylate	$\nu^a(CO_2^-)$	500
1598	Formate	$\nu^a(CO_2^-)$	100 to 400
	$CH_2NO_2^-$	ν(C=N)	100
1682	Carbamic acid	ν(CO)	300
2120	Cyanide	ν(CN)	300
2231	Isocyanate	$\nu(NCO^-)$	100 to 300
2250	Isocyanate	ν(NCO)	100 to 300
2905	Formate	ν(CH)	200 to 400
2959	Physisorbed NM		RT
3004	Formate	$\nu^a(CO_2^-) + \delta$(CH)	200 to 400
3067	$CH_2NO_2^-$	ν(CH)	RT
3192	$CH_2NO_2^-$	ν(CH)	RT

Figure 13 shows the DRIFT spectra of the species obtained following the adsorption of *tert*-butyl nitrite on 10% Ag/Al_2O_3. At low temperatures, i.e., 100 and 200°C, a wide plateau appeared between 1200 and 1700 cm^{-1}, and this made it difficult to identify the species absorbing in this region. However, two main peaks could be detected in this region at 1300 and 1558 cm^{-1}. Similar DRIFT spectra were obtained over 10% Ag/Al_2O_3 when NO and O_2 were fed to the catalyst and these two peaks were assigned to nitrate species (29, 35, 36). The stretching vibrations, ν(CH), of the *tert*-butyl group at 2975 and 2870 cm^{-1} were the other peaks detected on the sample surface at 100 and 200°C. At 300°C, nitrate species were the main surface species, while carboxylate species had begun to appear (peak at 1466 cm^{-1}). Increasing the temperature to 400°C resulted in the complete disappearance of the nitrate species and the presence of a single carboxylate species with characteristic symmetric and asymmetric stretching vibrations $\nu^s(CO_2^-)$ and $\nu^a(CO_2^-)$ at 1466 and 1575 cm^{-1}, respectively.

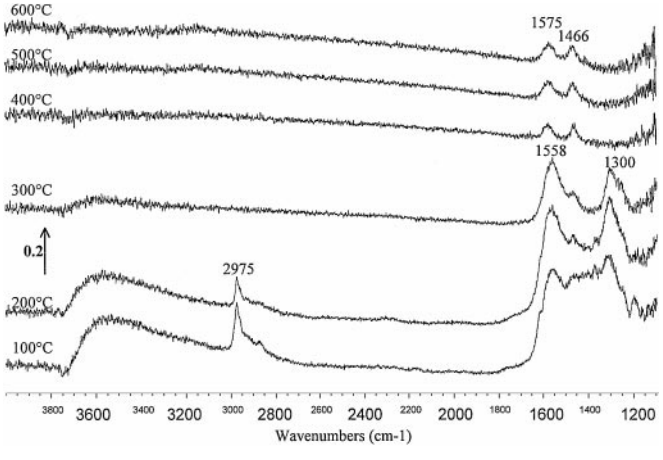

FIG. 13. *In situ* DRIFT spectra of the surface species resulting from the adsorption of *tert*-butyl nitrite on 10% Ag/Al_2O_3. Total flow = 100 ml min^{-1}.

Compared to the low silver loading material, less adsorption of alkyl species was observed on the 10% Ag/Al_2O_3 material, despite the higher concentration of Ag thought to enhance the HC adsorption capacity on the surface of the catalyst (Fig. 10). This is probably due to the difference in the nature of the Ag promoter, which is thought to be kept in an oxidised state at low loading, due to a greater dispersion and greater interaction with the alumina while metallic Ag particles are thought to predominate in the high loading material (37, 38).

3.5. *DRIFT Spectra on 0.4% Co/Al_2O_3*

The DRIFT spectra of the species formed on 0.4% Co/Al_2O_3 as a result of the adsorption of nitromethane are shown in Fig. 14. The spectra shown for each temperature are very similar to those obtained for the same reaction over unpromoted alumina (Fig. 4). The similarity between the unpromoted alumina and the 0.4% Co/Al_2O_3 sample can be attributed to the very low cobalt loading on alumina, which does not affect to any great extent the observable surface species.

TABLE 2

Assignment of the Bands Resulting from the Adsorption of *tert*-Butyl Nitrite on the Alumina-Based Materials (s = Symmetric, a = Asymmetric, ν = Stretching, δ = Bending)

Wavenumber (cm^{-1})	Surface species	Vibration	Temperature (°C)
1258	Nitrate NO_3^- "A"	ν^a(ONO)	300 to 500
1305	Nitrate NO_3^- "B"	ν^a(ONO)	100 to 400
1368	Tert-butyl	$\delta(CH_3)$	100
1476	Carboxylate	$\nu^s(CO_2^-)$	400 to 600
1556	Nitrate NO_3^- "A"	ν(N–O)	500
1571	Nitrate NO_3^-	ν(N–O)	100 to 400
	Carboxylate	$\nu^a(CO_2^-)$	400 to 600
1611	Nitrite	ν(N=O)	100
1689	Nitrite	ν(N=O)	100
2875	*tert*-Butyl	$\nu(CH_3)$	100
2975	*tert*-Butyl	$\nu(CH_3)$	100

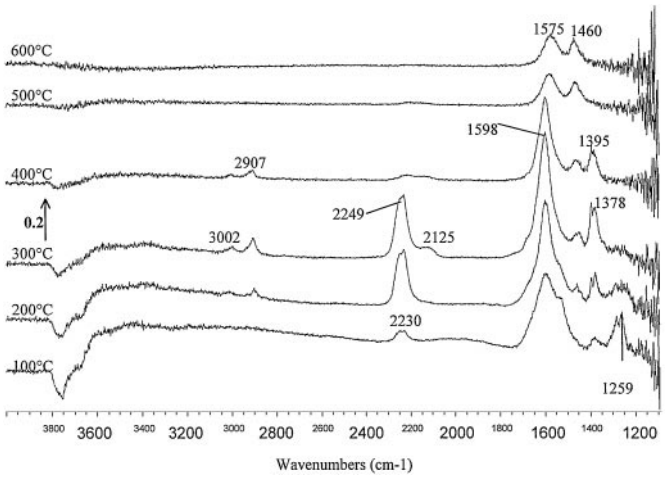

FIG. 14. *In situ* DRIFT spectra of the surface species resulting from the adsorption of nitromethane on 0.4%Co/Al_2O_3. Total flow = 100 ml min^{-1}.

Figure 15 shows the DRIFT spectra of the species formed from the adsorption of *tert*-butyl nitrite on 0.4%Co/Al_2O_3. As in the case of the adsorption of nitromethane on both unpromoted alumina and 0.4%Co/Al_2O_3 presented above, the spectra resulting from the adsorption of *tert*-butyl nitrite on 0.4%Co/Al_2O_3 were very similar to those obtained on alumina alone (Fig. 5). However, a difference could be observed: the higher reactivity (i.e., lower stability) of the nitrate species on the 0.4%Co/Al_2O_3 sample compared to the unpromoted alumina. These species had completely disappeared from the surface of the Co-containing sample at 400°C, while they were still present as the main surface species on alumina at this temperature. At higher temperatures, i.e., 500 and 600°C, the carboxylate species were again the only detectable species.

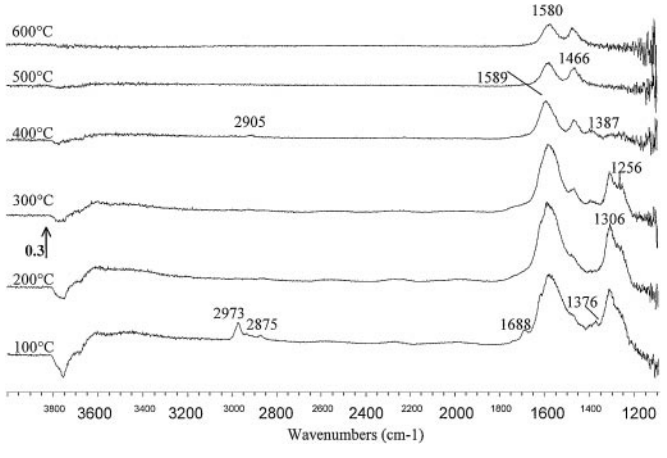

FIG. 15. *In situ* DRIFT spectra of the surface species resulting from the adsorption of *tert*-butyl nitrite on 0.4%Co/Al_2O_3. Total flow = 100 ml min^{-1}.

It appears from these results that the Co promoter is not involved in the reaction of the organo-nitrogen compounds as the catalytic data and DRIFT spectra obtained over the 0.4%Co/Al_2O_3 sample were similar to those obtained over unpromoted alumina. However, our group has previously reported that the presence of Co on alumina enhanced the rate of reaction of the C_3H_6-SCR of NO (26). Assuming that the C_3H_6-SCR of NO proceeds via the intermediacy of organo-nitro/nitrite-like species, this could suggest that the Co promoter would have a beneficial effect on one of the former steps of reaction, i.e., on the formation of the organo-nitrogen species rather than on their reaction.

3.6 Discussion

3.6.1. The reactivity of nitromethane over alumina-based materials. In agreement with the results reported by Yamaguchi (21), nitromethane ($H_3C{-}NO_2$) was found to dissociatively adsorb on the alumina surface at room temperature in its aci-nitro form. This process occurs as a result of tautomerisation of nitromethane to the corresponding oxime ($H_2C{=}N^+(O^-)OH$), followed by the reaction of the latter species over surface oxide sites. The resulting nitronate ion is then likely to be stabilised on the Lewis acid sites of the alumina, while the proton formed by dissociation would react on the basic sites of the oxide. The character amphoteric of the alumina could then explain the formation of the aci-anion of NM, which had been observed previously over basic alkaline earth oxide materials such as MgO and CaO and not over acidic oxides (39): despite its weaker basicity, Al_2O_3 enables the formation of aa-NM due to its amphoteric properties which allow the stabilisation of the anion on its Lewis acid sites. Increasing the temperature results in the reaction of this nitronate ion, which rearranges to form formohydroxamic acid, possibly through a three-membered cyclic oxaziridine intermediate as has been suggested by Blower and Smith (40). The formohydroxamic acid can then be hydrolysed to formates and hydroxylamine by the residual water present in the feed or, in contrast, it can be dehydrated to an isocyanate, in a reaction equivalent to the Lossen rearrangement of the O-acyl derivatives of hydroxamic acids (41). The formation of the isocyanate species from the nitro-compound might also occur through the dehydration of the enol tautomer of nitromethane to form fulminic acid species (HCNO), followed by isomerisation of this unstable nitrile N-oxide to give the isocyanate acid (HNCO) by a dyotropic rearrangement (42) (Fig. 16).

The formation of NH_3 from the oxidation of nitromethane could, hence, be explained by the thermal decomposition of nitromethane according to the following reaction steps:

$$CH_3NO_2 \rightarrow CHO{-}N(H)OH_{(ads)} \rightarrow HNCO_{(ads)} + H_2O \qquad [1]$$

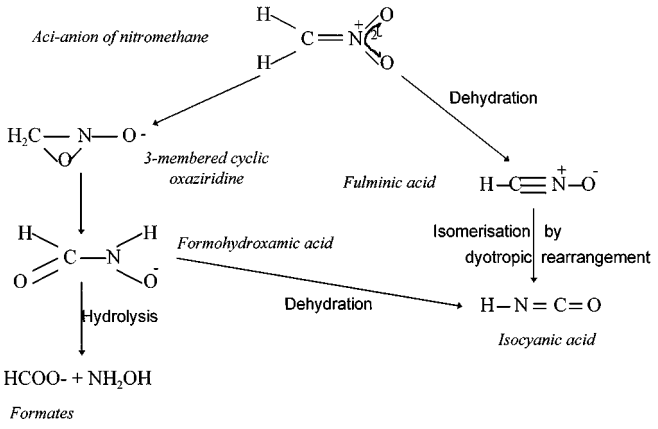

FIG. 16. Scheme of the reactivity of nitromethane over alumina.

$$HNCO_{(ads)} + H_2O \rightarrow NH_2COOH_{(ads)} \rightarrow CO_2 + NH_3. \quad [2]$$

The formation of NH_3 and CO_2 from the thermal decomposition of nitromethane in the presence of O_2 has been reported in the literature for various catalysts (18, 19, 43). The intermediacy of formohydroxamic acid species in Eq. [1] has already been suggested by Blower and Smith (40) and the suggestion is supported by the observation by DRIFTS in this work (Fig. 4) of IR bands at 1387 and 1533 cm^{-1}, which are compatible with the molecular structure of this surface species. The possible intermediacy of carbamic acid species in Eq. [2] is also supported by the observation by DRIFTS (Fig. 4) of IR bands at 1448 and 1681 cm^{-1}, those being compatible with its molecular structure. The decomposition of the latter would result in the formation of NH_3 and CO_2.

The reaction between the surface isocyanate species ($HNCO_{ads}$) and H_2O is probably fast enough on the Al_2O_3 surface to avoid the release of isocyanic acid (i.e., HNCO) to the gas phase, as no gaseous HNCO was detected during the catalytic oxidation experiment. This is in agreement with the results of Dümpelmann *et al.* (44, 45), who reported that alumina is a good catalyst for the hydrolysis of HNCO.

The formation of N_2 at temperatures above 400°C could be explained by the oxidation of NH_3 according to the following equation:

$$4NH_3 + 3O_2 \rightarrow 2N_2 + 6H_2O. \quad [3]$$

In a similar oxidation reaction, NO could be formed at these higher temperatures through the reaction of NH_3 with O_2:

$$4NH_3 + 5O_2 \rightarrow 4NO + 6H_2O. \quad [4]$$

HCN formation is believed to occur through two different pathways:

(i) The reaction of the possible reaction intermediate, formhydroxamic acid:

$$CHO{-}N(H)OH_{(ads)} \xrightarrow{+H_2O} HCOOH_{(ads)} + NH_2OH_{(ads)} \quad [5]$$

$$HCOOH_{(ads)} + NH_2OH_{(ads)} \xrightarrow[-H_2O]{} H_2C{=}N{-}OH \rightarrow HCN + H_2O. \quad [6]$$

The reaction of aldehydes with hydroxylamine is known to lead to the formation of oximes which can successively be dehydrated to give nitriles (46).

(ii) The reaction of surface formate species with gas phase ammonia to give formamide (NH_2CHO):

$$HCOOH_{(ads)} + NH_3 \rightarrow NH_2CHO + H_2O \quad [7]$$

$$NH_2CHO \leftrightarrow NH{=}CHOH \rightarrow HCN + H_2O. \quad [8]$$

The formamide can then rearrange to give its enol tautomer ($NH{=}CHOH$) whose dehydration results in the formation of HCN.

3.6.2. The reactivity of tert-butyl nitrite over alumina-based materials. *tert*-Butyl nitrite appears to react over alumina through the initial cleavage of its C–O bond to produce the *tert*-butyl carbocation which is stabilised on the O^{2-} sites of the oxide and the N-containing part of the molecule which reacts over the acid sites of the alumina to form nitrates (Fig. 17) (47).

The *tert*-butyl species adsorbed on the alumina are readily displaced with increasing temperature under argon, only nitrate species remaining on the sample surface at 300°C. Sadykov *et al.* (48) have previously reported that NO and NO_2 were formed in TPD experiments of nitrate species adsorbed on various catalysts, and so the formation of NO and NO_2 during the oxidation of *tert*-butyl nitrite could be explained using a similar mechanism. The nitrate species formed on the surface of the alumina sample from the adsorption of *tert*-butyl nitrite probably decomposes to produce the nitrogen oxides NO and NO_2. The formation of

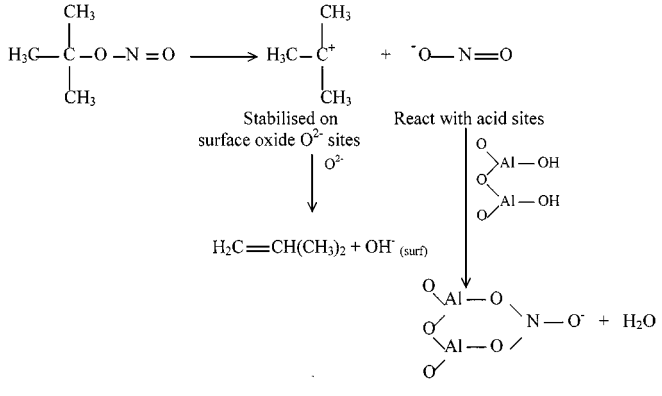

FIG. 17. Scheme of the reactivity of *tert*-butyl nitrite over alumina.

NH_3 and N_2 at temperatures above 300°C could be explained by the presence of large amounts of hydrocarbons, particularly methane and isobutene, produced during the reaction: these hydrocarbons can then function as reducing agents in the selective catalytic reduction of the nitrogen oxides (NO and NO_2) formed as primary products during the *tert*-butyl nitrite oxidation reaction.

3.6.3. Relation to the C_3H_6-SCR of NO over alumina. It clearly appears from those results that organo-nitro and organo-nitrite compounds react in a different way: while organo-nitro species mainly yield NH_3, organo-nitrite compounds can yield more NO_2. These observations could be related to the results previously reported on the C_3H_6-SCR of NO over promoted-alumina materials (24–26), where high yields of NO_2 (in excess of the thermodynamic limit associated with the direct oxidation of NO to NO_2 by O_2) were obtained over unpromoted alumina and 0.4%Co/Al_2O_3. From the results regarding the reactivities of nitromethane and *tert*-butyl nitrite over alumina, it appears that the compound from which the NO_2 originates during the C_3H_6-SCR of NO is more likely to be an organo-nitrite species rather than an organo-nitro one: nitromethane oxidation yielded mainly NH_3, which further reacted to produce N_2, no NO_2 being detected; on the other hand, *tert*-butyl nitrite yielded NO and NO_2 at low temperatures, the latter apparently reacting with the reducing agent present in the feed (isobutene) at higher temperatures. The formation of NH_3 observed in significant proportions during the C_3H_6-SCR of NO over alumina, but only when the conversion of propene was incomplete (24–26) could be explained through the intermediacy of an organo-nitro compound as NH_3 was obtained from reaction of nitromethane over alumina, as reported by Lombardo *et al.* (49) and confirmed here. NH_3 is a well-known reductant of NO and NO_2 under O_2-rich conditions over many catalytic materials (50). The intermediacy of NH_3 in the hydrocarbon-SCR reaction has been suggested for zeolitic catalysts (17, 51). Moreover, our group previously reported that NO_2 was observed only when NH_3 was absent and vice versa during the C_3H_6-SCR of NO (24–26). This observation was also made during the reactions of *tert*-butyl nitrite and nitromethane over alumina. These results strongly support the idea that a significant proportion of the N_2 formed during the C_3H_6-SCR of NO over alumina could arise from the reaction between NO_2 (formed from an organo-nitrite compound) and NH_3 (formed from an organo-nitro compound), or at least from the corresponding adsorbed species from which these molecules were formed (i.e., ad-NO_x, NO, and NO_2 for organo-nitrite compounds and $NCO_{(ads)}$ and NH_3 for organo-nitro compounds). A parallel route for N_2 formation may involve the reaction of NO with an adsorbed isocyanate species (i.e., $^-NCO + NO \rightarrow N_2 + CO_2$) similar to that proposed to be involved in CO/NO reaction over Rh catalysts (52).

3.6.4. The role of Ag in the reactivity of organo-nitrogen compounds and in relation to the SCR reaction. The isocyanate and cyanide species observed over the silver-promoted material during the C_3H_6-SCR of NO (24) could also be observed during the adsorption of nitromethane over alumina (Fig. 4) and 1.2%Ag/γ-Al_2O_3 (Fig. 8), the latter greatly promoting their formation compared to the unpromoted material. Isocyanate species were also detected on the sample surface during the adsorption of *tert*-butyl nitrite on 1.2%Ag/γ-Al_2O_3 (Fig. 9): the isocyanate and cyanide species observed over the silver-promoted material during the SCR reaction could be formed from species such as organo-nitro or nitrite compounds. Interestingly, the isocyanate band disappeared readily when the temperature was increased from 300 to 400°C, this temperature coinciding with the light-off temperature of the SCR reaction (24). On the other hand, the cyanide band was more stable. This suggests that the isocyanate species was the most reactive reaction intermediate. As our group has previously reported (24), the presence of Ag promotes the adsorption of ad-NO_x species compared to alumina alone during both the reaction of NO and O_2 and the selective catalytic reduction of NO by C_3H_6. The results reported here indicate that the presence of Ag also promotes the adsorption of HC species compared to unpromoted alumina. These observations could help explain the formation of isocyanate species on the 1.2%Ag/Al_2O_3 surface during the adsorption of *tert*-butyl nitrite (Fig. 9). Otsuka *et al.* (27, 28) reported that organo-nitro compounds were formed during the homogeneous partial oxidation of alkanes in the presence of NO and that organo-nitrite species played an important role as the intermediate of reaction. In a somewhat similar process, the *tert*-butyl nitrite under investigation here could rearrange to organo-nitro-like species: the higher surface coverage in HC and ad-NO_x species on the 1.2%Ag/Al_2O_3 sample could favour the formation of such organo-nitro compounds. Once the latter species are formed, it would be quite understandable that they could react to form "nitro-like-derived products" such as isocyanates (Eqs. [10] and [11]).

$$R{-}ONO \rightarrow HC_{(ads)} + NO_{x\,(ads)} \rightarrow R'\text{-}NO_2 \qquad [10]$$

$$R'\text{-}NO_2 \rightarrow \text{"Nitro-like derived products"} : NCO_{(ads)}. \qquad [11]$$

The promoting effect observed for the 1.2%Ag/Al_2O_3 during the C_3H_6-SCR of NO compared to unpromoted alumina seems characterised by an increased rate of formation of organo-NO_x compounds (resulting from a higher adsorption capacity of the Ag-promoted material for both ad-NO_x and hydrocarbon-like species).

3.6.5. The role of Co in the reactivity of organo-nitrogen compounds and in relation to the SCR reaction. The catalytic and DRIFT data reported in this work regarding

the reactivity of nitromethane and *tert*-butyl nitrite over 0.4%Co/Al_2O_3 are very similar to those obtained over unpromoted alumina. This seems to indicate that the Co promoter is not involved in the reaction of the organo-nitrogen compounds. However, kinetic data reported previously (26) showed that, as in the case of alumina, the NO_2 observed during the C_3H_6-SCR of NO over the 0.4%$Co/\gamma Al_2O_3$ material was not formed through the direct oxidation of NO by O_2. Moreover, the presence of Co on alumina was found to enhance the rate of reaction of the C_3H_6-SCR of NO (26). Assuming that the C_3H_6-SCR of NO proceeds via the intermediacy of organo-nitro/nitrite-like species as suggested for the unpromoted alumina, this could suggest that the Co promoter would have a beneficial effect on one of the former steps of reaction, i.e., on the formation of the organo-nitrogen species rather than on their reaction. Moreover, it was observed that, contrary to the cases of unpromoted alumina and 1.2%Ag/Al_2O_3, no NH_3 was observed over the 0.4%Co/Al_2O_3 sample during the C_3H_6-SCR of NO. This could suggest that the Co promoter would preferentially favour the formation of organo-nitrite compounds (from which NO and NO_2 originate) compared to the organo-nitro compounds (responsible for NH_3 formation): the proportion of oxidised nitrogen species produced was always greater than that of the reduced species and a large concentration of NO_2 therefore remained unreacted, this eventually decomposing back to NO and O_2. Overall, the promoting effect of cobalt seems to be explained by an increased rate of conversion of the reductant to an intermediate species such as an oxygenated compound which subsequently forms an organo-nitrito species by reaction with ad-NO_x species.

4. CONCLUSION

Organo-nitro and organo-nitrite compounds were found to react in a very different way over alumina-based catalysts. Nitromethane decomposed to isocyanate, cyanide, and formate species on the surface of the unpromoted alumina, 1.2wt%Ag/Al_2O_3, and 0.4wt%Co/Al_2O_3, the presence of Ag promoting the formation of isocyanate and cyanide species. In contrast, *tert*-butyl nitrite mainly gave rise to nitrate species on the surface of these catalysts. The oxidation of nitromethane over alumina, 1.2wt%Ag/Al_2O_3, and 0.4wt%Co/Al_2O_3, yielded NH_3 (resulting from the thermal decomposition of this compound) as main primary product of reaction, while the oxidation of *tert*-butyl nitrite over the same catalysts resulted in the formation of NO and (to a lower extent) NO_2 as main reaction products at low temperatures. Increasing the temperature led to the reaction of the primary products of reaction (NH_3 in the case of nitromethane and NO (and NO_2) in the case of *tert*-butyl nitrite) to give N_2 (among others).

The study of the reactivity of nitromethane and *tert*-butyl nitrite over alumina-based catalysts was then related to the observation that the formation of NO_2 during the C_3H_6-SCR of NO over γ-Al_2O_3 and 0.4wt%Co/Al_2O_3 was not achieved through the direct oxidation of NO by O_2 (24–26). The formation of NO_2 during the C_3H_6-SCR of NO over γ-Al_2O_3, and 0.4wt%Co/Al_2O_3 is suggested to involve the formation and combustion of organo-nitrito species, while NH_3 is suggested to derive from the reaction of organo-nitro species. Overall, the formation of N_2 during the C_3H_6-SCR of NO over γ-Al_2O_3, 1.2wt%Ag/Al_2O_3, and 0.4wt%Co/Al_2O_3 is proposed to occur through the reaction of organo-nitro compounds and/or their derivatives (e.g., isocyanate, cyanide, amines, and NH_3) with NO or the organo-nitrite and/or its derivative NO_2. The formation of organo-nitro compounds appeared to be promoted by a low loading of silver, while the presence of a cobalt promoter seems to favour the formation of organo-nitrite compounds.

ACKNOWLEDGMENTS

Part of this project was funded by the European Community, through the Environment and Climate Programme, subprogramme "Technologies for Rehabiliting the Environment," Contract ENV4-CT97-0658, and by Forbairt, Contract SC/1997/519.

REFERENCES

1. Burch, R., and Scire, S., *Appl. Catal. B* **3**, 295 (1994).
2. Li, Y., and Hall, W. K., *J. Phys. Chem.* **94**, 6145 (1990).
3. Burch, R., and Millington, P. J., *Catal. Today* **26**, 185 (1995).
4. Kikuchi, E., Yogo, K., Tanaka, S., and Abe, M., *Chem. Lett.* 1063 (1991).
5. Obuchi, A., Nakamura, M., Ogata, A., Mizuno, K., Ohi, A., and Ohuchi, H., *J. Chem. Soc. Chem. Commun.* **16**, 1150 (1992).
6. Hamada, H., Kintaichi, Y., Sasaki, M., and Ito, T., *Appl. Catal.* **70**, L15 (1991).
7. Hamada, H., *Catal. Today* **22**, 21 (1994).
8. Hamada, H., Kintaichi, Y., Inaba, M., Tabata, M., Yoshinari, T., and Tsuchida, H., *Catal. Today* **29**, 53 (1996).
9. Montreuil, C. N., and Shelef, M., *Appl. Catal. B* **1**, L1 (1992).
10. Shelef, M., Montreuil, C. N., and Jen, H. W., *Catal. Lett.* **26**, 277 (1994).
11. Masuda, K., Tsujimura, T., Shinoda, K., and Kato, T., *Appl. Catal. B* **8**, 33 (1996).
12. Tanaka, T., Okuhara, T., and Misono, M., *Appl. Catal. B* **4**, L1 (1994).
13. Bamwenda, G. R., Ogata, A., Obuchi, A., Oi, J., Mizuno, K., and Skrzypek, J., *Appl. Catal. B* **6**, 311 (1995).
14. Ukisu, Y., Miyadera, T., Abe, A., and Yoshida, K., *Catal. Lett.* **39**, 265 (1996).
15. Yokoyama, C., and Misono, M., *J. Catal.* **150**, 9 (1994).
16. Hayes, N. W., Joyner, R. W., and Shpiro, E. S., *Appl. Catal. B* **8**, 343 (1996).
17. Centi, G., Galli, A., and Perathoner, S., *J. Chem. Soc. Faraday Trans.* **94**, 5129 (1996).
18. Cowan, A. D., Cant, N. W., Haynes, B. S., and Nelson, P. F., *J. Catal.* **176**, 329 (1998).

19. Cant, N. W., Cowan, A. D., Doughty, A., Haynes, B. S., and Nelson, P. F., *Catal. Lett.* **46**, 207 (1997).
20. Obuchi, A., Wögerbauer, C., Köppel, R., and Baiker, A., *Appl. Catal. B* **19**, 9 (1998).
21. Yamaguchi, M., *J. Chem. Soc. Faraday Trans.* **93**, 3581 (1997).
22. Kameoka, S., Chafik, T., Ukisu, Y., and Miyadera, T., *Catal. Lett.* **51**, 11 (1998).
23. Zuzaniuk, V., Meunier, F. C., and Ross, J. R. H., *J. Chem. Soc. Chem. Commun*. 815 (1999).
24. Meunier, F. C., Breen, J. P., and Ross, J. R. H., *J. Chem. Soc., Chem. Commun*. **3**, 259 (1999).
25. Meunier, F. C., Breen, J. P., Zuzaniuk, V., Olsson, M., and Ross, J. R. H., *J. Catal.* **187**, 493 (1999).
26. Meunier, F. C., Zuzaniuk, V., Breen, J. P., Olsson, M., and Ross, J. R. H., *Catal. Today* **59**, 287 (2000).
27. Otsuka, K., Takahashi, R., Amakawa, K., and Yamanaka, I., *Catal. Today* **45**, 23 (1998).
28. Otsuka, K., Takahashi, R., and Yamanaka, I., *J. Catal.* **185**, 182 (1999).
29. Nakamoto, K., "Infrared and Raman Spectra of Inorganic and Coordination Compounds," 4th ed. Wiley-Interscience, New York, 1986.
30. Colthup, N. B., Daly, L. H., and Wiberley, S. E., *in* "Introduction to Infrared and Raman Spectroscopy," pp. 448–449. Academic Press, Boston, 1990.
31. Hayes, N. W., Grünert, W., Hutchings, G. J., Joyner, R. J., and Shpiro, E. S., *J. Chem. Soc. Chem. Commun*. 531 (1994).
32. Ukisu, Y., Sato, S., Muramatsu, G., and Yoshida, K., *Catal. Lett.* **16**, 11 (1992).
33. Busca, G., Lamotte, J., Lavalley, J. C., and Lorenzelli, V., *J. Am. Chem. Soc.* **109**, 5197 (1987).
34. Shen, Y., Suib, S. L., Deeba, M., and Koermer, G. S., *J. Catal.* **146**, 483 (1994).
35. Kijlstra, W. S., Brands, D. S., Poels, E. K., and Bliek, A., *J. Catal.* **171**, 208 (1997).
36. Schraml-Marth, M., Wokaun, A., and Baiker, A., *J. Catal.* **138**, 306 (1992).
37. Bethke, K. A., and Kung, H. H., *J. Catal.* **172**, 93 (1997).
38. Kung, M. C., Bethke, K. A., Yan, J., Lee, J. H., and Kung, H. H., *Appl. Surf. Sci.* **121**, 261 (1997).
39. Kheir, A. A., and Shaw, J. F., *J. Am. Chem. Soc.* **116**, 817 (1994).
40. Blower, C. J., and Smith, T. D., *Zeolites* **13**, 394 (1996).
41. March, J., "Advanced Organic Chemistry," 4th ed., p. 1093. Wiley, New York, 1992.
42. March, J., "Advanced Organic Chemistry," 4th ed. Wiley, New York, 1992.
43. Cant, N. W., Cowan, A. D., Liu, I. O. Y., and Satsuma, A., *Catal. Today* **54**, 473 (1999).
44. Dümpelmann, R., Cant, N. W., and Trimm, D. L., *J. Catal.* **162**, 96 (1996).
45. Dümpelmann, R., Cant, N. W., and Cowan, A. D., *Stud. Surf. Sci. Catal.* **101**, 1175 (1996).
46. March, J., "Advanced Organic Chemistry," 4th ed., pp. 906–1038. Wiley, New York, 1992.
47. Börensen, C., Kirchner, U., Scheer, V., Vogt, R., and Zelner, R., *J. Phys. Chem. A* **104**, 5036 (2000).
48. Sadykov, V. A., Baron, S. L., Matyshak, V. A., Alikina, G. M., Bunina, R. V., Rozovskii, A. Ya., Lunin, V. V., Lunina, E. V., Ivanova, A. N., and Veniaminov, S. A., *Catal. Lett.* **37**, 157 (1996).
49. Lombardo, E. A., Sill, G. A., d'Itri, J. L., and Hall, W. K., *J. Catal.* **173**, 440 (1998).
50. Bosch, H., and Janssen, F., *Catal. Today* **2**, 369 (1988).
51. Poignant, F., Saussey, J., Lavalley, J. C., and Mabilon, G., *Catal. Today* **29**, 93 (1996).
52. Mathyshak, V. A., and Krylov, O. V., *Catal. Today* **25**, 1 (1995).